

Multiple beam interference with near-grazing waves in dielectric wedges: monochromatic and polychromatic cases

G. Rodríguez Zurita^{1,2}, J. Pedraza-Contreras^{2,3}, R. Pastrana-Sanchez^{2,*}, A. Cornejo-Rodríguez³, and J.F. Vazquez-Castillo²

¹*Centro de Investigaciones en Óptica*

Apartado postal 1-948, 37000 León, Gto., Mexico

²*Facultad de Ciencias Físico-Matemáticas, Benemérita Universidad Autónoma de Puebla*

Apartado postal 1152, 72000 Puebla, Pue., Mexico

³*Instituto Nacional de Astrofísica Óptica y Electrónica*

Apartado postal 51, 72000 Puebla, Pue., Mexico

Recibido el 11 de diciembre de 1996; aceptado el 13 de diciembre de 1997

Optical waves with wave vectors making an angle close to $\pi/2$ with the normals of two parallel, dielectric plates (near-grazing waves) contribute to total fields whose phase are step-wise nearly constant as a function of the gap between plates. This feature makes possible for near-grazing waves to generate multiple beam interference patterns in dielectric wedges under monochromatic or even polychromatic illumination. A transfer function is proposed to describe both cases and some of its consequences are numerically investigated. Chromatic tendencies of the derived interference patterns with inclusion of dispersion effects are shown for several glass types. Experimental observations are also presented.

Keywords: Interference patterns, dielectric wedges

Las ondas ópticas con vectores de onda formando ángulos cercanos a $\pi/2$ con cualquier normal de dos placas dieléctricas plano-paralelas contribuyen a campos totales cuyas fases son, escalonadamente, casi constantes. Esta característica hace posible que las ondas cuasi-rasantes generen patrones de interferencia en cuñas dieléctricas, tanto bajo iluminación monocromática como policromática. Se propone una función de transferencia para describir ambos casos y algunas de sus consecuencias son investigadas numéricamente. Las tendencias cromáticas derivadas, con inclusión de efectos dispersivos, son mostradas para algunos tipos diferentes de vidrio. Se presentan también observaciones experimentales.

Descriptores: Patrones de interferencia, cuñas dieléctricas

PACS: 42.25.H; 07.60.L; 78.66; 82.80.C

1. Introducción

It has been reported that several remarkable bright interference patterns appear when a beam of monochromatic light impinges one of the cathetus faces of a rectangular prism at an incidence angle within a suitable range, provided that the prism's hypotenuse face is placed close to an almost planar surface, thus forming a wedge [1]. Multiple beam interference of near-grazing waves has been recognized as responsible for that interference effect (near-grazing waves are traveling waves having wave vectors forming an angle of nearly $\pi/2$ with the normal of one of the wedge's faces). Accordingly, two properties of near grazing waves contribute to the pattern formation: their high reflectivity (close to unity even without highly reflective coatings) and their relative weak dependence of phase as a function of the gap between reflective surfaces. This last property has been pointed out by Carniglia and Mandel while inspecting the phase dependence of evanescent waves on gaps between two parallel plates [2].

Each one of the referred interference patterns can thus be thought of as a pattern resulting from multiple reflections within a wedge (as multiple-beam fringes within thin

films [3]), but with the particular attribute that the waves playing the important role are just near-grazing waves. Considering their weak phase dependence property, it is expected that they could carry readily observable consequences when employing polychromatic illumination. Polychromatic interference fringes with opposite contrast can indeed be obtained showing wide fringes (whether dark or bright), thus forming a pattern basically different from the well known white-light interference pattern arising by two interfering polychromatic beams. This fact makes possible a multibeam interferometer with white light. Also, the system results very stable due to the tolerance of near-grazing waves to gap changes.

Because the interference effect can be observed under conditions very close to those needed for applications and situations involving optical tunneling [4], evanescent waves [5], the Goos-Hänchen effect [6], the Imbert effect [7], and other dielectric interface phenomena [8, 9], it can be of some value to have a better understanding of its properties. In spite of these relations and the easy observation of the fringes, no mention of such an effect seems to be found in the literature as far as we know, neither so an attempt to describe its properties. Along this communication, a transfer function to de-

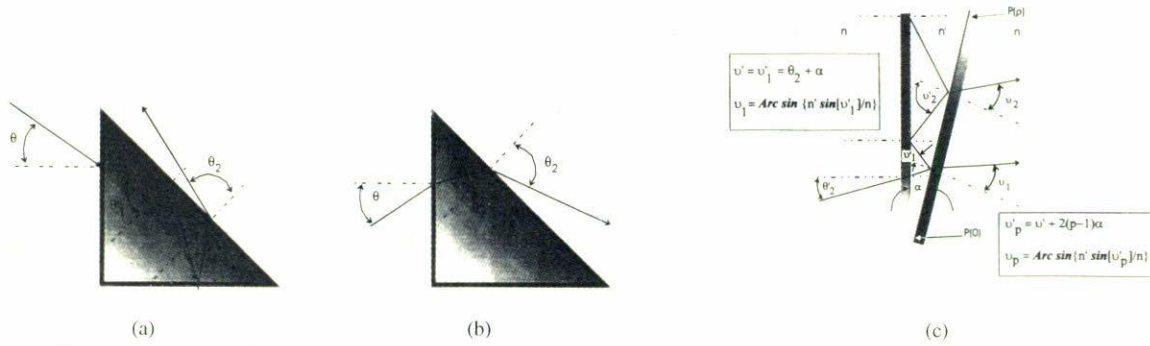


FIGURE 1. θ : entrance angle. θ_2 : propagation angle of transmitted waves. (a) Near-grazing waves generation after two reflections. (b) Near-grazing waves generation before any reflection. (c) Multiple beam reflections in a wedge. ρ : position from the apex.

scribe multibeam interference with near-grazing waves in a dielectric wedge (*s* polarization) is proposed. Numerical results under variations of relevant parameters are shown. Monochromatic and polychromatic illumination are numerically investigated and experimental observations to test the main general consequences of the transfer function are also reported. The analysis of the *p* polarization case would require of similar considerations as for the *s* polarization presented. Incorporation of the respective Fresnel coefficients and additional *E*-field components calculations would be needed.

2. Multibeam interference with near-grazing waves

2.1. Near-grazing waves generation with right angle prism

Near-grazing waves can be generated with bundles of rays entering to one of the surfaces of a prism at entrance angles θ having a given range of values. Two possible orientations of entrance angles at incidence angle θ impinging one of the cathetus faces of a rectangular prism are shown in Figs. 1a and 1b. It is an easy matter to check out that, for case (a)

$$\theta'_1 = \pi/4 + \theta_1, \tag{1}$$

where $n \sin \theta = n' \sin \theta'$. Also, for both case (a) and case (b), the following relation,

$$\theta'_2 = \pi/4 - \theta_1, \tag{2}$$

holds. Then, there exists incidence angles θ belonging to rays which impinge a cathetus face, such that $\theta'_2 < \theta_c$, θ_c being the critical angle. As a consequence, for such values of θ , the corresponding values of θ_2 must be close to $\pi/2$ (Fig. 1). This means that the emerging traveling wave is a near-grazing wave. On the contrary, note that in Fig. 1a, $\theta'_1 > \theta_c$, in agreement with Eq. (1) (total internal reflection, TIR). Reflections at this angles give rise to evanescent fields at the external side of the face of incidence. Their possible contributions are not taken into account along this discussion,

Prisms normally designed to work with TIR can be employed to generate near-grazing waves by deviating slightly enough the entering angles from their usual values.

2.2. Multiple reflections within a dielectric wedge

Figure 1c shows a wedge with an angle α formed by two dielectric surfaces. Following Ref. 3, successive reflection angles obey the relationships

$$\nu'_p = \nu' + 2(p - 1)\alpha, \tag{3}$$

where $\nu' = \nu'_1 = \theta_2 + \alpha$. Also, the phase difference for the *p*-reflection is

$$\delta_p = (4\pi\lambda)n'\rho \{ \sin[(p - 1)\alpha] \cos \nu' \} \{ \cos[(p - 1)\alpha] - \tan \nu' \sin[(p - 1)\alpha] \} + 2(p - 1)\phi, \tag{4}$$

where ρ is the coordinate position of a point $P(\rho)$ and ϕ a possible phase shift due to reflection. In general, the refractive indexes n and n' are functions of λ .

Considering dielectric reflections, Fresnel coefficients of reflection and transmission $r(\nu)$ and $t(\nu)$ can be used for each reflection, taking specially into account their respective angle dependence. By using $r'(\nu')$ and $t'(\nu')$ for reflection and transmission during reflections within the medium of index n' , the phase shifts are included over the Stokes relations, and there is no need of carrying ϕ . For the total amplitude $A^{(t)}$ on each point $P(\rho)$ over one face, we arrive to the following relation

$$A^{(t)} = A^{(i)} t(\nu) \sum_{p=1}^N \left\{ t'[\nu' + 2(p - 1)\alpha] \times \prod_{q=0}^{2(p-1)} r'(\nu' + q\alpha) \right\} \cos \delta_p, \tag{5}$$

(where $A^{(i)}$ denotes the entrance amplitude) and the corresponding normalized interference pattern or transfer function would be given by

$$I(\rho, \lambda) = |A^{(t)}/A^{(i)}|^2 \tag{6}$$

Equation (5) reduces to the equivalent transfer function for multiple beam Fizeau interference in case of constant coefficients of reflection and transmission [3].

2.3. Chromatic calculations

2.3.1. Dispersion Relations

To define Eq. (6) as a function of λ properly, calculation of refractive indexes are needed. The dispersion formula

$$n^2 = A_0 + A_1\lambda^2 + A_2\lambda^{-2} + A_3\lambda^{-4} + A_4\lambda^{-6} + A_5\lambda^{-8} \tag{7}$$

can be used to that end, where λ is expressed in μm . The same refractive index are assumed for both dielectrics making the wedge. Values of the coefficients are to be found in [10].

2.3.2. Chromatic Relations

The CIE-1931 calorimetric system can be used to describe the tendencies in chromaticity predicted by Eq. (6). Thus, the following relations for the tristimulus values are employed

$$\begin{aligned} X(\rho) &= \sum_{\lambda} I(\rho, \lambda) S(\lambda) \underline{X}(\lambda), \\ Y(\rho) &= \sum_{\lambda} I(\rho, \lambda) S(\lambda) \underline{Y}(\lambda), \\ Z(\rho) &= \sum_{\lambda} I(\rho, \lambda) S(\lambda) \underline{Z}(\lambda), \end{aligned} \tag{8}$$

with \underline{X} , \underline{Y} , and \underline{Z} the color matching function of the standard colorimetric observer, $S(\lambda)$ the spectral radiance distribution of a standard illuminant, and the sums are carried out at 5 nm wavelength interval. Chromatic coordinates (x, y) are to be derived from Eqs. (8) as usual [11].

3. Numerical results

Along these sections, numerical results corresponding to both monochromatic and polychromatic cases are presented after using the formulae previously described. θ denotes the entrance angle at one face of the prism in whatever case squelched in Fig. 1a or Fig. 1b. Both wedge surfaces are assumed to have the same refractive index. Refractive index for the wedge was taken as unity.

3.1. Monochromatic case

3.1.1. Examples with BK7 glass type

As a typical glass, the appropriate values for BK7 glass type were used and the C line (656.3 nm) employed. Experimental observations with a laser beam and two prisms suggest that 5 reflections can be taken as a typical reflection number. Figure 2 shows the comparison between a two-beam interference pattern and Eq. (6) for a wedge with $\alpha = 0.008$ deg. Although the optical path differences produce several fringes

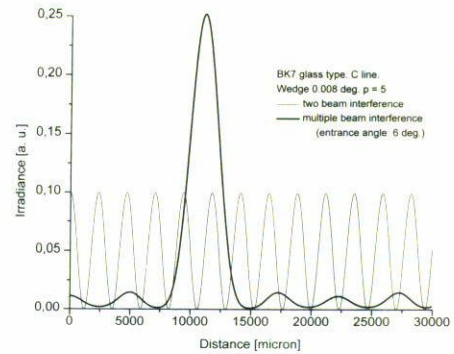


FIGURE 2. Comparison between two interference patterns for the same wedge angle ($\alpha = 0.008^\circ$). ρ : distance.

in two beam interference, there is only one isolated peak within the same ρ -range for the near-grazing case ($\theta = 6^\circ$). Secondary maxima also appear in this interference pattern.

For another value of α (0.06°), Fig. 3a shows how the multibeam pattern evolves as the entrance angle changes around the threshold entrance angle (angle at which condition expressed as $\theta'_2 < \theta_c$ begins to hold): fringes density grows with the entrance angle θ , and so the irradiance of maxima. This irradiance, however, reaches a maximum and then begins to fall, as the Fig. 3b shows for a wider entrance angle range for the first 6 brighter orders. The order positions of the first 5 orders decay as a function of θ so that they can be approximated as an exponential fit (best with two exponentials), as can be seen at the Fig. 3c. They depart at most for higher θ -values. Each order position follows a linear relation for a constant entrance angle (Fig. 3d).

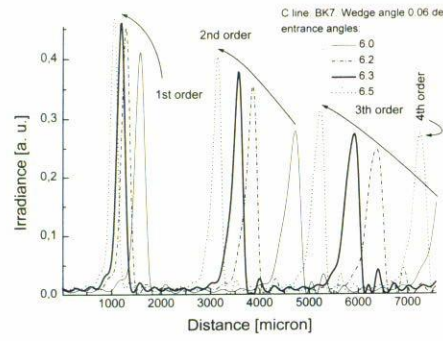
3.2. Polychromatic case

3.2.1. Chromatic tendencies and dispersion influence

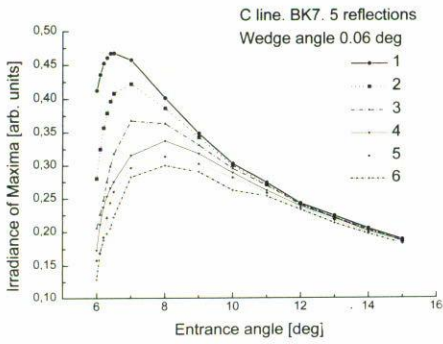
As a global test to inspect the dependence of polychromatic patterns on dispersion, four different glass types were chosen with different principal refraction indexes (n_e) and Abbe numbers (ν_e) so that they appear opposite when plotted at the $(n_e - \nu_e)$ diagram. The chosen glass types were accordingly the following [10]: BK7 (1.51859–63.87), F8 (1.59910–38.95), LASF (1.83427–29.87) and SFS 1 (1.93322–20.79). In order to have entrance angles as low as possible, the range of wavelengths in calculations were limited from 490 to 705 nm. As the distribution $S(\lambda)$, the standard illuminant C was used [11].

The polychromatic multibeam patterns for each glass type are to be seen at the Fig. 4. Threshold entrance angles are different due to the n_e values. The range of angles where the fringes begin to loss contrast also differs in each case. It is wider for the lower Abbe number.

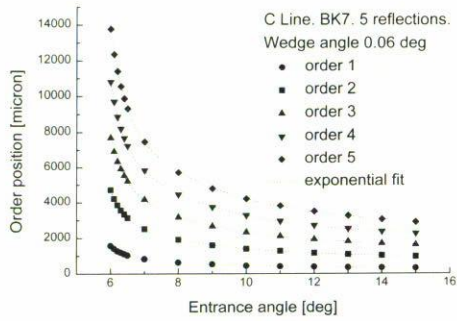
Following Kubota [12], the evolution of the color of the polychromatic patterns as they run between the first and the third peak (close to threshold conditions) were plotted in the CIE-1931 chromaticity diagram as shown in Fig. 5. Figure 5a



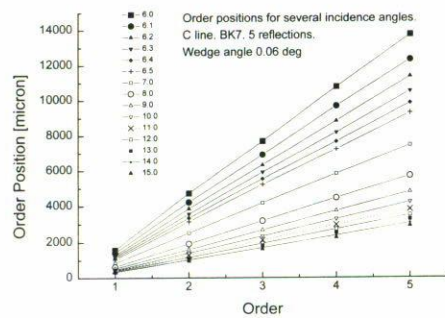
(a)



(b)

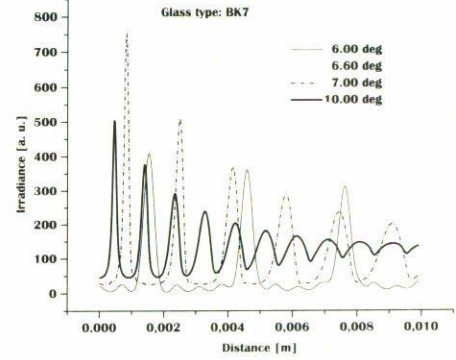


(c)

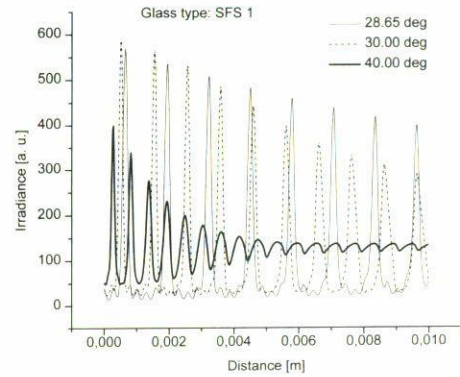


(d)

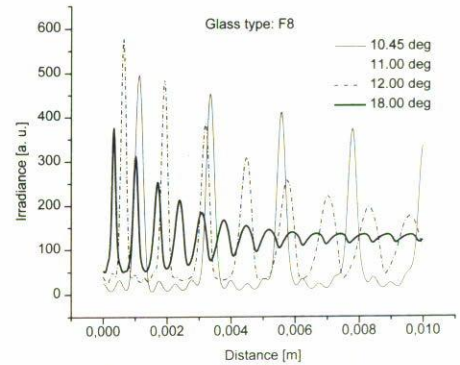
FIGURE 3. Peaks properties of multibeam interference patterns for BK7 ($\alpha = 0.06^\circ$). Monochromatic case (C line). (a) Patterns for several θ -values. (b) Irradiance of maxima as a function of θ . (c) Order position as a function of θ . (d) Order position as a function of order.



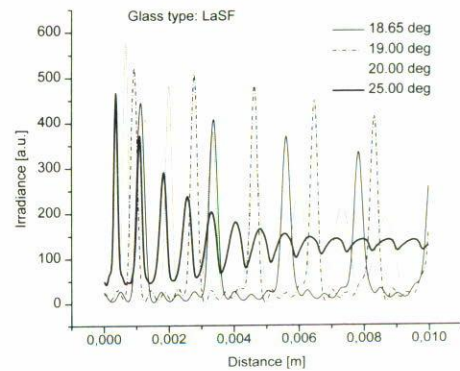
(a)



(b)



(c)



(d)

FIGURE 4. Near-grazing waves multibeam interference patterns for several glass types. Polychromatic case ($\alpha = 0.06^\circ$). (a) BK7. (b) SFS 1. (c) F8. (d) LaSF.

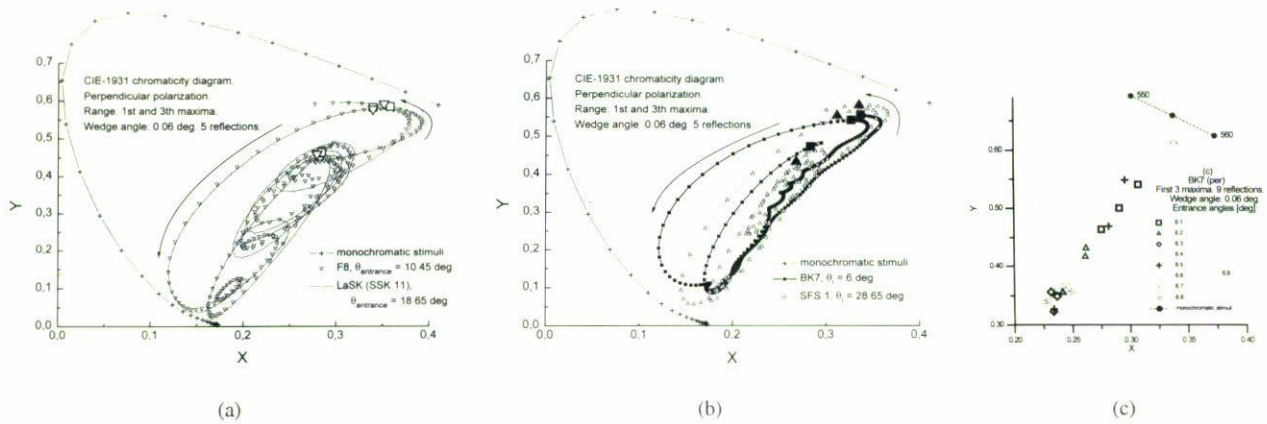


FIGURE 5. Chromaticity tendencies of polychromatic patterns ($\alpha = 0.06^\circ$). Color coordinates (x, y) belonging to maxima are enhanced with bigger point symbols for several glass types. (a) F8 and LaSK. (b) BK7 and SFS 1. (c) Color coordinates of the three maxima and several entrance angles (BK7 only).

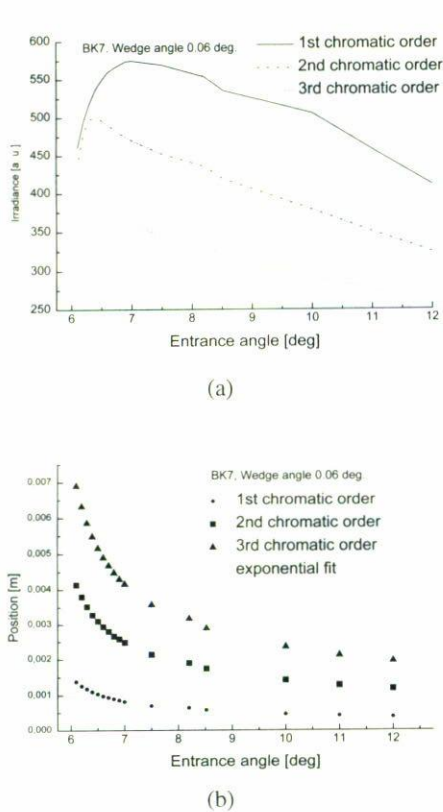


FIGURE 6. Peaks properties of multibeam interference patterns for BK7 ($\alpha = 0.06^\circ$), polychromatic case. (a) Irradiance of chromatic maxima as a function of θ . (b) Order position as a function of θ .

includes the traces of F8 and LaSK, where a very similar chromatic tendency can be noted. There are even regions of overlapping and each pair of color coordinates, for each of the three maxima, are very close one to each other (at both sides of the frontier between the yellowish-green and yellow-green regions). The respective tendencies for BK7 and SFS 1

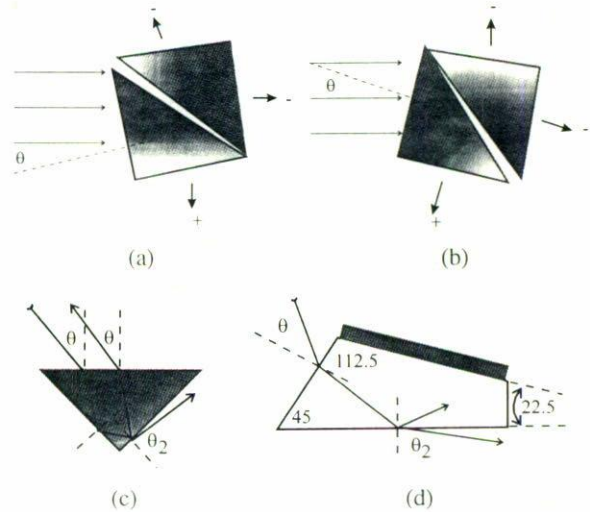


FIGURE 7. Array of prisms to observe multibeam interference patterns. (a) According to Fig. 1a. (b) According to Fig. 1b (-), contrast in transmission; (+), contrast in reflection. (c) Near-grazing waves generation with a Porro prism. (d) Same with a 45-112.5-22.5 prism.

are not as similar as the previous case, and the color coordinates of the maxima differ more, as Fig. 5b shows. This results suggest that the dispersion have great influence on the chromatic tendency. In all plots, the third order color tends to saturate more than the second and the first one.

Figure 5c presents the color coordinate changes for the three first maxima as the entrance angle θ changes just after threshold conditions for BK7, and with 9 reflections Colors spread about a line connecting the yellow-green and the less saturated blue-green region. Except for $\theta = 6.8^\circ$, the third and second peak color coordinates are close to each other. Besides the irradiance distribution, the color tendencies are markedly different than that presented by Kubota for two beam interference [12].

3.2.2. Polychromatic fringes in BK7

The irradiance values of the three lower polychromatic peaks as a function of the entrance angle θ (Fig. 6a) show a maximum for certain angle as in the monochromatic case (Fig. 3b), although the curves are not as regular. The position values of the same polychromatic orders become lower as the entrance angles increase (Fig. 6b), just as in the monochromatic case (Fig. 3c). Exponential approximations fits the points.

4. Experimental observations

A number of observations can be performed with pairs of prisms in arrangements mounted on rotating stages following the sketches of, Figs. 7a and 7b. Three interference patterns can be observed along the directions indicated by arrows. A fourth pattern is to be seen towards the light source. The contrast of each pattern is denoted by (-) whenever displays sharp bright peaks against wider, dark backgrounds. The opposite contrast is denoted by a (+) sign. Thus, the plots of irradiance previously presented have contrast with (-) sign. The contrast of the fourth pattern is (+). The orientation of the wedge apex has to be as shown, so that the wave's propagation angles grow as they travel leaving behind the apex.

Otherwise, the angles tend to be smaller and the waves won't be near-grazing ones.

For the configuration of Fig. 7a (entrance as Fig. 1a), it can be of convenience to reinforce the partial internal reflection with a reflective metallic film [1]. However, fringes appear also without such reflecting deposition.

The angles of observation of the beginning of the effect under laser illumination (He-Ne 632.8 nm) are $6^{\circ} 5' \pm 5'$ using a pair of BK7 prisms with hypotenuse faces in close contact. There is uncertainty in the exact value to be taken under polychromatic illumination mainly due to the fact that some of the wavelengths included in the beam enter the wedge at lower entrance angles than others. Monochromatic and polychromatic fringes can be seen also with Porro prisms, or with 45-112.5-22.5 prisms in several configurations. Figures 7c and 7d indicate how near-grazing waves can be generated with those prisms.

4.1. Monochromatic case

Figure 8 shows the basic set-up to compare multibeam interference patterns with Fizeau interference patterns at the same time. A laser source, the cube beam-splitter and the entrance prism, keep their relative position but are able to rotate as a whole in order to change the entrance angle of a second beam from another collimated source (whether laser or white light), which remains fixed. In this situation, the multibeam pattern has opposite contrast as the calculated because it is formed with waves leaving the wedge to its left. Figure 9 presents three pairs of photos of the patterns arising from different adjustments of the surfaces making the wedge. The recordings

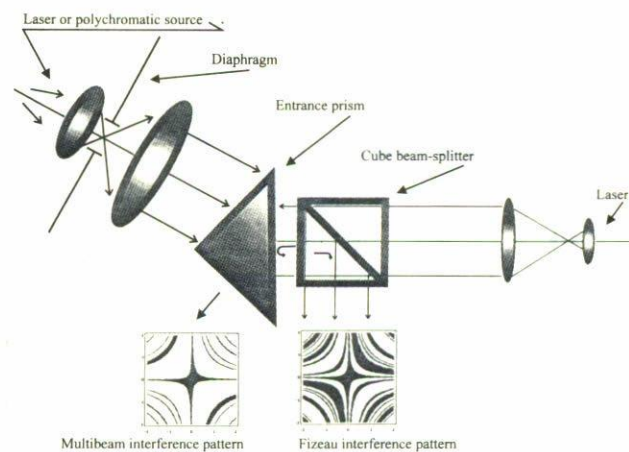


FIGURE 8. Experimental set-up to observe multibeam and Fizeau patterns from the same wedge.

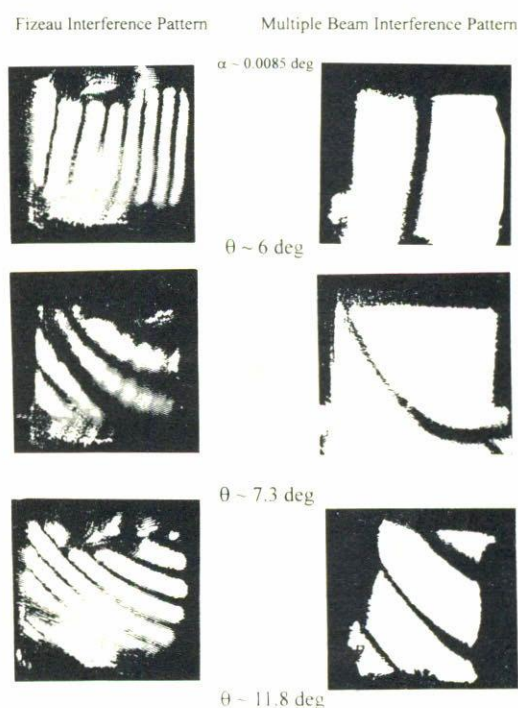


FIGURE 9. Some Fizeau and corresponding multibeam patterns (monochromatic case, $\lambda = 632.8$ nm).

were taken without camera objective. The first pair of photos from above shows the patterns of a wedge of $\alpha = 0.0085^{\circ}$ according with the Fizeau pattern, so the pair can be compared against the Fig. 2. Remembering the contrast change, there is an agreement with the respective fringes densities. Readjustment of the surfaces leads to a change in the fringe distribution and there is no more a wedge in general, but the fringe shapes correspond in each related pattern.

Measurement of fringe position as a function of the entrance angle are shown for two neighboring orders in, Fig. 10.

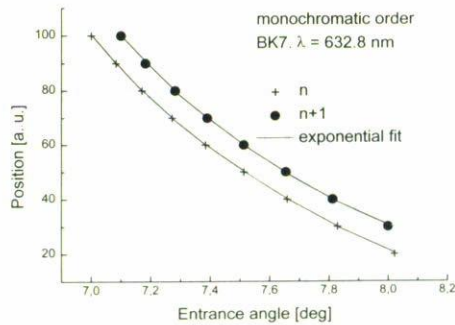


FIGURE 10. Experimental order position as a function of θ .

The data admit an exponential fit good. Measurements of angles were carried out with a rotating stage with minimum scale graduation in 5° .

4.2. Polychromatic case

Instead of a laser source, a collimated xenon lamp source was used to illuminate a pair of rectangular prisms forming the wedge with their respective hypotenuses. The use of a source other than a C standard source represents a factor which can lead to discrepancies between calculated and observed colors. The prism pair was mounted on a rotating stage, and observation of fringes of opposite contrast could be performed.

Figure 11 shows recording of polychromatic fringes with opposite contrast for the same wedge. The higher the entrance angles, the higher the fringe density. The polychromatic fringes differ from the white-light two-beam interference pattern because there are wide regions of dark fringes (or white fringes according to the contrast). Colors of opposite contrast are, at least in tendency, complementary. By following the first fringe formed under threshold conditions, the first peak can be identified. In the patterns with ample dark bands (*i.e.*, with [-] contrast), this peak appears as a yellowish line in our recording. It corresponds itself to a bluish-purple line for the case of opposite contrast. Both lines are narrow.

Noteworthy enough, the fringe colors are not symmetrical about the yellowish narrow line. We attribute this color distribution to the fact that, for beams of finite width, dispersion (*via* refraction) makes separate beams traveling at different angles from the entrance face on. Therefore, beams of different wavelength become displaced one from each other. This occurs not only within the wedge, but also after reflection.

An example is in order. For beams just entering the wedge, the longer wavelengths travel at higher angles. Thus, there are regions in the edge of the beam which does not have contributions from lower wavelengths, which accounts for the lack of blues and violets in the red and green maxima at one side of the yellowish line. Calculations did not take this effect into consideration.

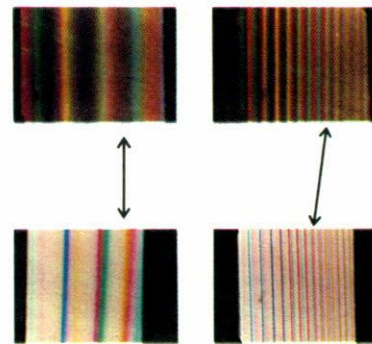


FIGURE 11. Polichromatic multibeam interference patterns at two different entrance angles θ . Top patterns (-) contrast, bottom patterns (+) contrast.

5. Final comments

Several aspects of multiple beam interference are still in current research [13]. The properties of near-grazing waves can lead to one of these aspects, namely, highly contrasted interference patterns with sharp fringes. We have shown that this interference effect can be observed under monochromatic as well as polychromatic illumination. Interference fringes can be achieved under diverse conditions and their appearance is predictable on the basis of near-grazing waves. The weak phase dependence of near-grazing waves seems to explain the observation of chromatic interference patterns with polychromatic light sources, even when the wedge film is not thin enough so as to be able to produce chromatic interference fringes at zero incidence (Fizeau fringes of equal thickness with white light). Demonstration of some properties of near-grazing waves interference are thus easily achieved with thick films (films of several wavelengths thick) under white light, collimated illumination (which includes sunlight).

The proposed transfer function includes reflections dependent on incidence angles and dispersion effects. It shows tendencies which qualitatively explain several features of the observed patterns. Their dependence on dispersion has properties which can found applications in dispersion characterization. The influence of evanescent waves in the patterns remains to be searched.

Acknowledgments

One of the authors (GRZ) is in leave of absence at CIO from the Universidad Autónoma de Puebla. This work was partially supported by CONACyT (grant codes 3649E and 92984).

- ‡. Estudiante del Instituto Nacional de Astrofísica Óptica y Electrónica
1. J. Pedraza-Contreras, G. Rodríguez-Zurita, A. Cornejo-Rodríguez, and O. Cardona- Nuñez, *Rev. Mex. Fis.* **40** (1994) 7.
2. C.K. Carniglia and L. Mandel, *J.O.S.A. A* **61** (1971) 1035.
3. M. Born and E. Wolf, *Principles of Optics*, Fifth edition (Pergamon Press, Oxford, 1975), p. 351.
4. N.F. van Huist, F.B. Segefink, and B. Bolger, *Opt. Commun.* **87** (1992) 212.
5. O. Bryngdahl, in *Progress in Optics*, vol. XI (North-Holland Publishing Co., Amsterdam, 1973), p. 169.
6. F. Bretenaker, A. Le Floch, and L. Dutriaux, *Phys. Rev. Lett.* **68** (1992) 931.
7. C. Imbert, *Phys. Rev. D, third series* **5** (1972) 787.
8. H. Osterberg and L.W. Smith, *J.O.S.A.* **54** (1964) 1073.
9. T. Tamir and A.A. Oliner, *J.O.S.A.* **59** (1969) 942.
10. *Optisches Glas*, Katalog 011S. VEB JENAer Glaswerk Schott & GEN., JENA DDR.
11. G. Wyszecki and W.S. Stiles, *Color Science. Concepts and methods, quantitative data and formulae*, 2nd edition (Wiley, New York, 1982).
12. H. Kubota, in *Progress in Optics*, vol I (North-Holland Publishing Co., Amsterdam, 1961), p. 213.
13. T.T. Kajava, H.M. Lauranto, and A.T. Friberg, *J.O.S.A. A* **11** (1994) 2045.